Available online at www.sciencedirect.com
SCIENCE DIRECT®
Journal of Crystal Growth 269 (2004) 592–598
JOURNAL OF CRYSTAL GROWTH
www.elsevier.com/locate/jcrysgro

Local control of the dendritic microstructure through perturbation

K. Lee*, W. Losert

Department of Physics, IPST, and IREAP, University of Maryland, College Park, MD 20742, USA

Received 15 October 2003; accepted 6 May 2004

Available online 17 June 2004

Communicated by M.E. Glicksman

Abstract

The spacing between cells and dendrites in directional solidification of binary alloys is analyzed and controlled experimentally. An organic alloy analogue with laser dye allows in situ imaging and perturbations of the cell and dendrite structure. Perturbations permit accurate control of the microstructure, either by guiding the initial formation of the pattern or by triggering subcritical transitions between stable microstructures. This control of microstructure through perturbation allows us to investigate the modes of instability of crystal growth patterns.

PACS: 81.30.Fb; 68.70.+w; 47.20.Hw

Keywords: A1.Dendrites; A1.Directional solidification; A1.Morphological stability

This experimental study focuses on control of microstructures which develop during directional solidification of binary alloys. In directional solidification, the material is solidified by pulling it through a temperature gradient. For dilute binary alloys the solid–liquid interface is planar at low pulling speeds, and forms cellular and dendritic arrays at increasing speed [1]. The shape of this interface is reflected in the microstructure of the resulting alloy, and influences the material properties of the alloy. Changes in pulling speed, temperature gradient, or alloy composition provide coarse control of the microstructure, but often only to within a factor two or less and with great uncertainties at transitions between patterns such as the cell-dendrite transition, since they often exibit strong hysteresis. Here we demonstrate that a local perturbation technique can provide accurate control of the microstructure. We show that this technique also provides valuable quantitative data on microstructure stability.

A schematic phase diagram based on experimental observations [2,3] and consistent with

*Corresponding author. Tel.: +1-301-405-6759; fax: +1-301-405-1678.

E-mail addresses: kyuyong@wam.umd.edu (K. Lee), wlosert@glue.umd.edu http://www.ireap.umd.edu.

0022-0248/$ - see front matter © 2004 Elsevier B.V. All rights reserved.
doi:10.1016/j.jcrysgro.2004.05.021

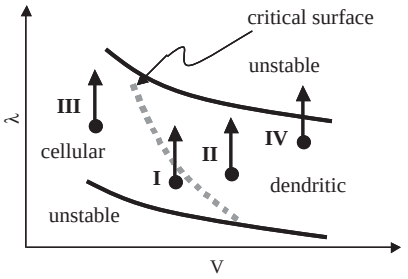

Fig. 1. Schematic phase diagram of the solid–liquid interface pattern as a function of growth speed V and interdendritic spacing λ.

numerical results [4,5] is shown in Fig. 1. It shows the solid–liquid interface pattern as a function of growth speed V and interdendritic spacing λ. A range of λ of cellular and dendritic arrays is stable at a given V, and the stable λ decreases with increasing V. The transition from stable cellular to dendritic regions (critical surface marked as a dotted line) was found to be supercritical [6]. Within the range of stable λ, the selected λ and structure exhibit strong hysteresis [7]. The arrows I, II, III, and IV indicate transitions from one state to another, and will be discussed below.

Our study shows how λ can be selected in a controlled way at the start of solidification, and how it can be adjusted dynamically. The investigation focuses on the regime close to the cell to dendrite transition, where dendrites interact strongly with each other.

As an alloy model system, we use the organic crystal Succinonitrile (SCN) with the laser dye Coumarin152 (C152) added in small concentration of 0.31 wt% [1]. C152 can absorb sufficient energy under UV light or laser illumination to locally heat the sample. This local heating perturbs the interface pattern and thus the C152 concentration field as explained in more detail in Refs. [1,8]. Such local perturbations through heating were first employed in solidification experiments by Qian and Cummins [9]. We use UV light spots (100 W mercury lamp) with controlled masks that generate UV light patterns or up to 200 independently moveable laser spots from a holographic laser tweezer to locally heat the sample (Bioryx200 from Arryx Inc.,0.2−2 W total power, 532 nm). The sizes of the heated region depends on the magnification of the microscope objective, through which both UV and laser light is guided to the sample. Laser spot sizes are of the order of 10 μm and UV spot sizes are 65−350 μm with 4× magnification objectives.

We study a 100 μm × 2 mm × 20 cm sample filled and sealed under vacuum. In our study the temperature gradient G is varied from 4.4 K/cm to 30.2 K/cm, and the pulling speed, which is the same as the crystal growth speed V in steady state, is varied from 0.9 to 31.0 μm/s.

We emphasize that we use thermal perturbations to control an interface whose shape is otherwise determined from solute diffusion. In order to allow the solute field to adjust to the altered interface shape, it is hence necessary to apply the perturbations for some time comparable to the solute diffusion time between two laser spots, i.e. of order 1 min for 200 μm separated spots. This approach should generally work if the perturbation is applied long enough to allow adjustment of the solute field.

Planar to pattern transitions: The best time to control λ of cellular or dendritic arrays accurately is during the inital instability, when crystal growth starts. Here, we selectively heat regions in the liquid ahead of the solid–liquid interface by applying a row of uniformly spaced UV spots while the interface undergoes a planar to dendritic transition (Fig. 2). The UV light spots have Gaussian intensity profile with width of about a quarter of the distance between the spots, which effectively form a sinusoidal perturbation. We have not yet investigated the dependence on spot size systematically, but we find that for spot sizes much smaller than the spacing between spots (e.g. using laser spots), the resulting interdendritic spacing becomes less uniform. Simulations and theoretical analyses have indicated that for optimal control of the shape of the planar front perturbations should be applied a distance of the order of the diffusion length ahead of the front [10]. Here, even though we want to trigger a controlled instability, we also find that positioning the UV perturbations approximately one diffusion length (45 μm at $V = 10$ μm/s) ahead of the interface works best. The position of UV spots is

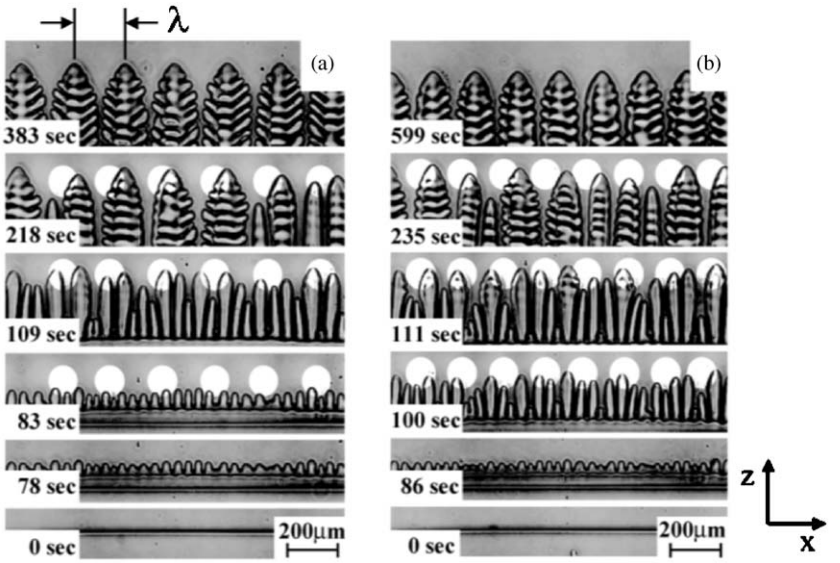

Fig. 2. Uniform dendritic arrays with controlled interdendritic spacing λ are obtained through spatially periodic UV perturbations (bright spots). UV spots: (a) spacing 235 μm, Gaussian width 70 μm, duration 247 s, (b) spacing 190 μm, Gaussian width 65 μm, duration 434 s.

manually adjusted in the z-direction, but fixed in the x-direction. Although the UV spots heat the sample by less than ~ 0.2 K($<0.1\%$ of the melting temperature and $<1.2\%$ of the latent heat/specific heat ratio of SCN) the dendrites align between UV spots and form a regular array. When the perturbation is removed, the dendritic array remains uniform and stable. Different λ can be selected by varying the spacing of UV spots. Through such perturbations any λ in the stable regime of the phase diagram can be accurately selected.

With time an initially broad distribution of λ of the order of the wavelength of the planar instability changes into a sharp distribution peaked at the spacing imposed by the UV spot array. The standard deviation of interdendritic spacings $\delta\lambda$ (Fig. 3a) for the controlled arrays approaches nearly zero while $\delta\lambda$ for the non-controlled array decreases more slowly and stays far from zero. In general, the appropriate number of dendrites is established at an early stage before $\delta\lambda$ reaches a steady state as the system adjusts λ continuously (Fig. 3b). This influence of control on λ is more useful in dendritic arrays at low temperature gradients, where the range of stable λ is broad due to the strong interaction between sidebranches [2].

Pattern to pattern transitions: Transitions from one stable pattern to another are also possible. Fig. 4a shows an array of cells close to the cell to dendrite transition. This pattern is stable; small perturbations like the ones applied to a planar front are no longer sufficient to control the microstructure. Instead, large perturbations are needed to alter the microstructure as shown in Fig. 4. Under strong spatially periodic perturbation of every other cell a transition to a stable dendritic array is observed (Fig. 4c). This corresponds to the transition I in Fig. 1.

The necessary perturbation strength can be quantified from the response to small perturbations [11]. Fig. 5 shows a plot of the modulation amplitude ξ, i.e. the difference in tip position between perturbed and unperturbed cells (see Fig. 4a), after perturbations of various strengths are applied to every other tip. A third order amplitude equation suffices to characterize the time evolution of ξ during this cell–dendrite transition:

$$\frac{d\xi(t)}{dt} = a_0\xi(t) + a_1|\xi(t)|^2\xi(t). \quad (1)$$

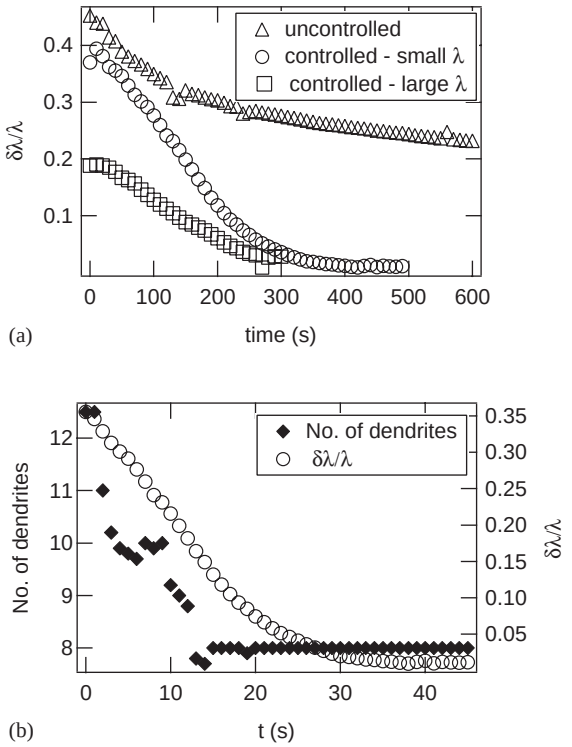

Fig. 3. (a) The standard deviation of interdendritic spacings $\delta\lambda$ decreases to zero more rapidly under perturbations than in a reference experiment without perturbation. (same run as in Fig. 2; small and large λ correspond to (a) and (b), respectively) (b) The number of dendrites reaches a steady state at an early stage while $\delta\lambda$ shows continuous adjustment toward uniform λ before and after that ($G = 7.5\,\mathrm{K/cm}$, $V = 8.8\,\mu\mathrm{m/s}$).

Here a_0 and a_1 are linear and third order growth coefficients, respectively. Both a_0 and a_1 depend on the wavelength of the perturbation (i.e. the spacing between UV spots) and the spacing between cells or dendrites, but do not depend on the strength of the perturbation.

Small ξ decay exponentially. When ξ starts above a critical value, ξ grows with time, leading to the period doubling transition shown in Fig. 4 (note that the third order amplitude equation can

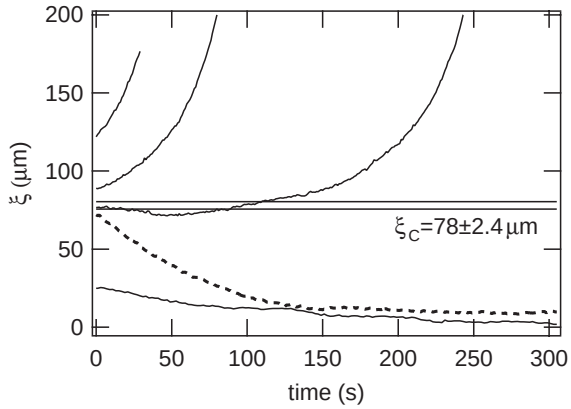

Fig. 5. Modulation amplitude ξ vs time after perturbations with different strength. The band indicates the critical amplitude with uncertainty. The bottom two lines show weak perturbation, which lead to a decaying ξ. The top three lines show the growth of ξ (which leads to period doubling) after strong perturbations. ($G = 4.4\mathrm{K/cm}$, $\mathrm{V} = 5.9\,\mu\mathrm{m/s}$).

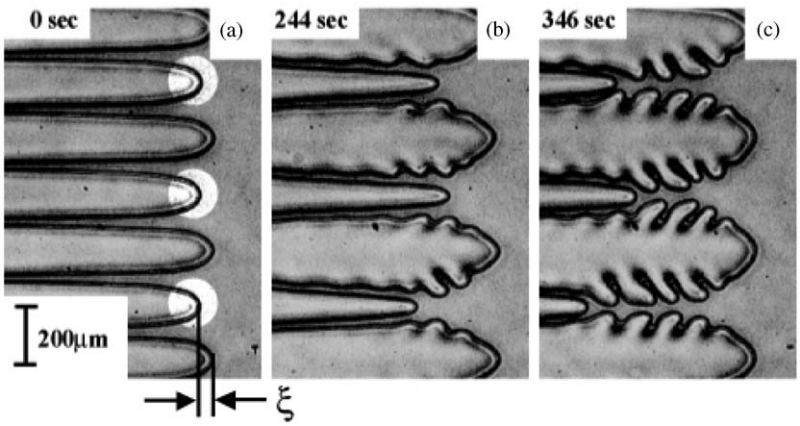

Fig. 4. Guiding the crystal growth pattern through perturbations: a stable cellular interface pattern (a) is perturbed through localized perturbation of every other tip (UV spots: spacing 386 μm, Gaussian width 96 μm, duration 40 s). This triggers a transition (b) to another stable microstructure, a dendritic array (c).

only describe that inital amplitudes above a critical threshold grow, and does not capture the transition to a new stable pattern). The critical initial amplitude from Eq. (1) is given by $\xi_C = \sqrt{-a_0/a_1}$. Nonlinear fitting of the decaying ξ for the dashed line shown in Fig. 5 yields a value of $\xi_C = 78.4\,\mu m$ (shown as a band), in good agreement with the amplitude at which perturbations grow.

Other transitions: It is also possible to trigger a transition from a stable dendritic array to a period doubled dendritic array as indicated by the arrow II in Fig. 1. Experimentally transitions to other than period doubled patterns require stronger perturbations, which is not surprising since period doubling has been found to be the most unstable mode of the system [12].

In addition, a period halving transition from a dendritic to a cellular array can be triggered through very strong UV perturbation on every tip but this transition is less accurately controllable (Fig. 6).

We could not trigger a cell to cell transition in several experiments in a parameter range, which corresponds to the transition III in Fig. 1, where one might most likely expect such a period doubling instability. This observation, and the visual indication e.g. in Fig. 4b that sidebranches prevent the perturbed cells from recovering, point to the important role of sidebranches for array stability and selection. We will present other experimental results in support of this assumption in detail elsewhere [13].

Transient structures: Perturbations can also transiently generate microstructures with unsustainably large or small λ (for example, the transition IV in Fig. 1). This allows us to study what instability modes limit the range of stable λ. In Fig. 7 dendritic and cellular arrays are forced to have λ larger than the upper limit of stable spacings λ_{Max} under spatially periodic perturbation of every other dendrite or cell.

For dendrites λ is limited above λ_{Max} by sidebranches that lead to additional dendrites, an instability that is preceeded by sideway tip oscillations (Fig. 7a). For cells, λ is limited by a tip splitting instability (Fig. 7b). For both cells and dendrites, a period doubling instability provides a minimum stable λ_{Min}. Through repeated perturbations on cellular or dendritic arrays of different interdendritic spacing, the perturbation technique can indicate the range of stable λ and the mode of instability (e.g. oscillatory or tip splitting).

Non-periodic structures: Control of non-periodic microstructures requires more complex spatio-temporal perturbations. For our model alloy, a new holographic laser tweezer system provides up to 200 independently movable laser spots. Fig. 8 shows the laser spots applied to a cellular front. Through appropriate positioning and motion of the perturbation points, we continuously increase the local interdendritic spacing λ around a dendrite or a cell in an array. When the local λ reaches a threshold value, the array reduces λ by either growing sidebranches or tip splitting. The

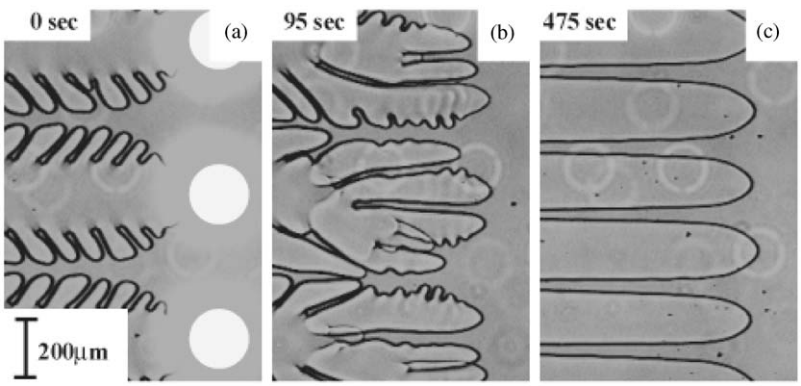

Fig. 6. A period halving transition from a dendritic to a cellular array is triggered through very strong UV perturbation on every tip. UV spots: spacing 386 μm, Gaussian width 96 μm, duration 76 s.

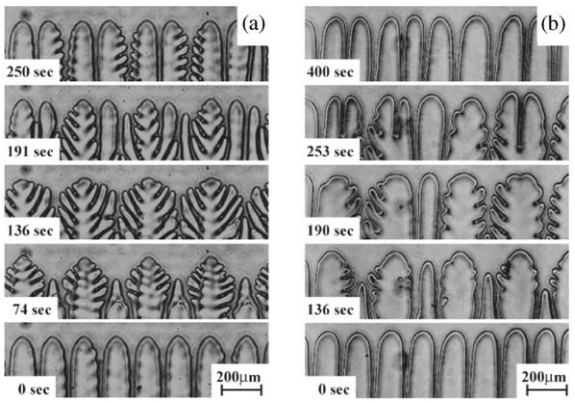

Fig. 7. Arrays with λ larger than the stable range can be generated transiently through perturbations (second image from below) but the unstable array returns to smaller λ by growing sidebranches (left) or tip splitting (right).

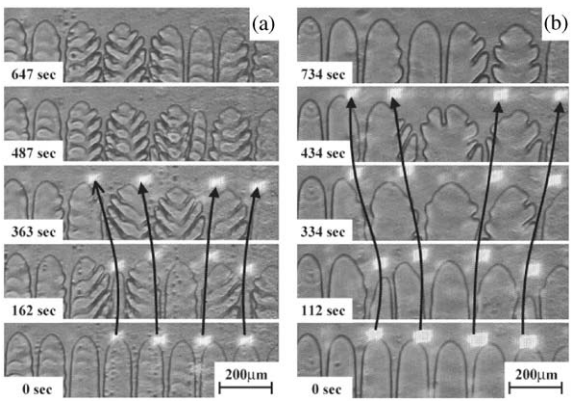

Fig. 8. Control of non-periodic structures: the local λ is continuously increased by independently movable laser spots (40 μm in diameter) until the system adjusts λ through instabilities— (a) sidebranch growing and (b) tip splitting. The arrows indicate the controlled motion of laser spots.

critical λ where these instabilities occur is in good agreement with λ_{Max} obtained by the method of step-increase of the growth speed [2]. This indicates that in our parameter range of strongly interacting dendrites, array stability is mostly determined by nearest neighbor interactions.

In summary, we have studied experimentally how to use thermal perturbations to accurately control solute diffusion generated cellular and dendritic arrays in directional solidification of a model binary alloy SCN-C152. Spatially periodic thermal perturbations during the initial instability create controlled arrays of cells or dendrites with any desired interdendritic spacing in the stable range. Large perturbations can trigger a transition from one stable state to another stable state. Finally, perturbations allow us to temporarily trigger λ that is outside of the stable range. This has allowed us to find tip splitting and side-branching as the modes of instability at λ greater than λ_{Max}, and period doubling instabilities at λ smaller than λ_{Min}. Holographic techniques are used to generate controlled, non-periodic structures.

Recent experimental results point to the possibility of controlling real metallic alloys using similar techniques. Global perturbations through pressure pulses might be sufficient for control of periodic microstructures by exploiting temporal resonances [14]. X-ray imaging of dendritic growth has provided in situ imaging of pattern formation [15]. We thus anticipate that the control and analysis techniques shown in this paper could be applied to metallic alloys using interference patterns of X-rays of a wavelength that gets partially absorbed, or using other means of perturbations that can penetrate the material such as ultrasound or microwave radiation.

Acknowledgements

We would like to thank H.Z. Cummins for the experimental setup and collaboration on initial experiments. We thank A. Karma and J.A. Warren for valuable discussions and suggestions. This work was supported by a Research Corporation Research Innovation award, NSF-MRSEC grant DMR-00-80008 at the University of Maryland, and NASA grant NNM04AA15G.

References

[1] W. Losert, B.Q. Shi, H.Z. Cummins, Proc. Nat. Acad. Sci. USA 95 (1998) 431.
[2] W.D. Huang, X.G. Geng, Y.H. Zhou, J. Crystal Growth 134 (1993) 105.
[3] S.H. Han, R. Trivedi, Acta Metall. Mater. 42 (1994) 25.
[4] S.Z. Lu, J.D. Hunt, J. Crystal Growth 123 (1992) 17.
[5] B. Echebarria, A. Karma (unpublished).

[6] M. Georgelin, A. Pocheau, Phys. Rev. E 57 (1998) 3189.
[7] M.A. Eshelman, V. Seetharaman, R. Trivedi, Acta Metall. 36 (1988) 1165.
[8] W. Losert, D.A. Stillman, H.Z. Cummins, P. Kopzcynski, W.-J. Rappel, A. Karma, Phys. Rev. E 58 (1998) 7492.
[9] X.W. Qian, H.Z. Cummins, Phys. Rev. Lett. 64 (1990) 3038.
[10] T.V. Savina, A.A. Nepomnyashchy, S. Brandon, D.R. Lewin, A.A. Golovin, J. Crystal Growth 240 (2002) 292.
[11] W. Losert, O.N. Mesquita, J.M.A. Figueiredo, H.Z. Cummins, Phys. Rev. Lett. 81 (1998) 409.
[12] W. Losert, B.Q. Shi, H.Z. Cummins, J.A. Warren, Phys. Rev. Lett. 77 (1996) 889.
[13] K. Lee, W. Losert (unpublished).
[14] M.B. Koss, J.C. LaCombe, M.E. Glicksman, V. Pines, A. Chait, Presentation at the 2002 Materials Science Conference, Huntsville Alabama June 25–26 2002.
[15] R.H. Mathiesen, L. Arnberg, F. Mo, T. Weitkamp, A. Snigirev, Phys. Rev. Lett. 83 (1999) 5062.